Research

New Phytologist

Fibre-specific regulation of lignin biosynthesis improves biomass quality in *Populus*

Jinshan Gui[1], Pui Ying Lam[2], Yuki Tobimatsu[2], Jiayan Sun[1], Cheng Huang[1], Shumin Cao[1,3], Yu Zhong[1,3], Toshiaki Umezawa[2] and Laigeng Li[1]

[1]National Key Laboratory of Plant Molecular Genetics and CAS Center for Excellence in Molecular Plant Sciences, Shanghai Institute of Plant Physiology and Ecology, Chinese Academy of Sciences, Shanghai 200032, China; [2]Research Institute for Sustainable Humanosphere, Kyoto University, Uji, Kyoto 611-0011, Japan; [3]University of the Chinese Academy of Sciences, Beijing 100049, China

Authors for correspondence:
Laigeng Li
Tel: +86 21 54924151
Email: lgli@sibs.ac.cn

Toshiaki Umezawa
Tel: +81 774 38 3625
Email: tumezawa@rish.kyoto-u.ac.jp

Jinshan Gui
Tel: +86 21 54924161
Email: jsgui@sibs.ac.cn

Received: *4 September 2019*
Accepted: *27 December 2019*

New Phytologist (2020) **226:** 1074–1087
doi: 10.1111/nph.16411

Key words: biomass, cell wall, fibre cell, lignin, *Populus*, wood formation.

Summary

- Lignin is a major component of cell wall biomass and decisively affects biomass utilisation. Engineering of lignin biosynthesis is extensively studied, while lignin modification often causes growth defects.
- We developed a strategy for cell-type-specific modification of lignin to achieve improvements in cell wall property without growth penalty. We targeted a lignin-related transcription factor, *LTF1*, for modification of lignin biosynthesis. LTF1 can be engineered to a nonphosphorylation form which is introduced into *Populus* under the control of either a vessel-specific or fibre-specific promoter.
- The transgenics with lignin suppression in vessels showed severe dwarfism and thin-walled vessels, while the transgenics with lignin suppression in fibres displayed vigorous growth with normal vessels under phytotron, glasshouse and field conditions. In-depth lignin structural analyses revealed that such cell-type-specific downregulation of lignin biosynthesis led to the alteration of overall lignin composition in xylem tissues reflecting the population of distinctive lignin polymers produced in vessel and fibre cells.
- This study demonstrates that fibre-specific suppression of lignin biosynthesis resulted in the improvement of wood biomass quality and saccharification efficiency and presents an effective strategy to precisely regulate lignin biosynthesis with desired growth performance.

Introduction

Wood is an important carbon-neutral biomass for production of timber products, paper pulping, chemicals and biofuels. In terms of anatomy, wood is structured mainly with thickened secondary cell walls, which primarily consist of cellulose impregnated with hemicelluloses and lignin (Kumar *et al.*, 2016). Being a major component of wood, lignin is a phenolic polymer, providing cell walls with fortified mechanical strength and hydrophobicity for upright growth and transportation of water and nutrients through the vascular system (Whetten & Sederoff, 1995).

The main building blocks of lignin are three monolignols, that is *p*-coumaryl, coniferyl and sinapyl alcohol, which are polymerised via oxidative coupling into *p*-hydroxyphenyl (H), guaiacyl (G) and syringyl (S) units in lignin polymers, respectively. Lignin composition varies considerably among plant taxa and species (Boerjan *et al.*, 2003). For example, lignin in gymnosperms is mainly composed of G units, whereas lignin in angiosperm dicots consists principally of G and S units (Boerjan *et al.*, 2003). In monocots, especially in grasses, lignin incorporates G and S units partially decorated with γ-acyl groups (e.g. γ-*p*-coumarates and ferulates) along with tricin flavonoid units (Lam *et al.*, 2019; Ralph *et al.*, 2019). Typical gymnosperm and dicot lignins contain very low or undetectable levels of H units, whereas monocot lignins tend to incorporate larger amounts of H units, albeit at still low levels (Lapierre, 1993; Gui *et al.*, 2011). As different types of lignin monomers can form different types of intermonomeric linkages in lignin polymers (Ralph *et al.*, 2019; Tobimatsu & Schuetz, 2019), the composition of lignin monomers is likely to be the key determinant of various properties of lignin and cell walls as a whole. It is believed that lignin composition varies among different cell types, such as in vessels and fibres (Boerjan *et al.*, 2003; Nakashima *et al.*, 2008), although the quantitative determination of cell-type-specific lignin composition is still challenging.

Conversely, presence of lignin in cell walls imparts recalcitrance in deconstruction of the wall materials for pulping and biofuel production (Weng *et al.*, 2008; Pauly & Keegstra, 2010). To reduce such cell wall recalcitrance, a great deal of interest has been invested to engineer lignin to reduce lignin content or modify lignin composition (Li *et al.*, 2003; Chen & Dixon, 2007; Leple *et al.*, 2007; Shadle *et al.*, 2007; Voelker *et al.*, 2010; Gui

et al., 2011; Eudes *et al.*, 2012; Van Acker *et al.*, 2014; Umezawa, 2018; Wang *et al.*, 2018). However, the lignin-modified plants often exhibit growth defects which consequently affect biomass production, thus limiting the benefits of lignin modification (Chen & Dixon, 2007; Voelker *et al.*, 2010; Gui *et al.*, 2011; Bonawitz *et al.*, 2014; Van Acker *et al.*, 2014). Therefore, developing optimised strategies to manipulate lignin biosynthesis without yield penalty is crucial for overcoming the adverse effects of lignin modification on plant growth.

Lignin biosynthesis-related transcription factor 1 (LTF1), belonging to the R2R3-MYB subfamily, binds to the promoter of lignin biosynthesis genes to represses lignin biosynthesis in *Populus* (Gui *et al.*, 2019). Several members in this subfamily across various plant species are reported to play a role in regulation of lignin biosynthesis (Zhao & Dixon, 2011; Rao & Dixon, 2018; Rao *et al.*, 2019). *LTF1* shares a high degree of sequence homology with *AtMYB4* in Arabidopsis, which is involved in regulation of the phenylproponoid metabolism pathway (Jin *et al.*, 2000). In *Populus*, LTF1 can be phosphorylated in response to external stimuli, however the phosphorylation sites are not conserved in AtMYB4 (Gui *et al.*, 2019). The phosphorylated LTF1 is degraded which leads to the release of its suppression on lignin biosynthesis and thus the phosphorylation-null LTF1 can convey a persistent suppression of lignin biosynthesis. In this study, we developed a new strategy to modify lignin biosynthesis through a cell-type-specific control of the expression of phosphorylation-null LTF1. The engineered LTF1 was introduced into *Populus* under the control of vessel-specific and fibre-specific promoters, respectively. Fibre-specific suppression of lignin biosynthesis resulted in improvement of biomass quality without growth defects. In-depth lignin analysis of the transgenics with cell-type-specific lignin modification revealed new insights into how cell-type-specific lignin biosynthesis is related to plant growth.

Materials and Methods

Plant transformation, growth conditions and morphological analysis

Populus deltoides × *P. euramericana* cv 'Nanlin895' was used in this study. About 2 kb of the *PdXCP1* (Potri.004G207600) promoter region and 1.8 kb of the *PdDUF579-9* (Potri.005G141300) promoter region (Song *et al.*, 2014) were cloned from *Populus*. After sequencing, the correct promoter fragments were fused with the 35S minipromoter (regions from −90 to + 8) (Benfey & Chua, 1990) and subcloned into a *pCAMBIA2300-GUS* vector upstream of *uidA* (GUS). The constructed *pCAMBIA2300:PdDUF579-9p-35S mini-GUS* and *pCAMBIA2300:PdDUF579-9p-35S mini-GUS* vectors were transferred into *Agrobacterium* strain GV3101 for *Populus* transformation. For cell-type-specific expression of phosphorylation-null *LTF1* (*LTF1*^{AA}) in *Populus*, the full-length of *LTF1* (Potri.004G174400) was mutated to *LTF1*^{AA} and fused with the tag 3Flag and then subcloned into binary vectors *pCAMBIA2300:PdXCP1p-35S mini-GUS* and *pCAMBIA2300:PdDUF579-9P-35S mini-GUS*, respectively. Primers used in this study are listed in Supporting Information Table S1. The obtained *pCAMBIA2300:PdXCP1P-35S mini-LTF1*^{AA}*-3Flag* and *pCAMBIA2300:PdDUF579-9P-35S mini-LTF1*^{AA}*-3Flag* vectors were mobilised into *Agrobacterium* strain GV3101 for genetic transformation according to the procedure (Li *et al.*, 2003).

Trees were grown in a phytotron under conditions of 60% relative humidity, 12 h photoperiod at 9000 lux, and 24°C constant temperature during young stage, and then grown in a glasshouse for a further characterisation or transplanted in a field at Shanghai (Crop cultivation and breeding station, Shanghai Institute of Plant Physiology and Ecology) (39.937128°N, 121.122304°E) for field test (from March 2018 to March 2019). Trees were clonally propagated through cutting and their morphological parameters, including plant height, stem diameter, internode length, leaf blade length and width, and petiole length were measured in 2-month-old trees. Plant height was determined as the shortest distance between shoot tip and stem base; stem diameter was measured 5 cm up from the stem base; internode length, leaf blade length and width and petiole length were measured from the 11th to the 20th internodes counted from the shoot top.

Gene expression analysis

Total RNA was extracted from the stem of *Populus* at the 2-month-old stage using a total RNA kit following the manufacturer's instructions (Omega). Transcript levels of *LTF1* and secondary cell wall biosynthesis-related genes were determined, as described previously, using a MyiQ Real-time PCR System (Bio-Rad). The gene expression data were normalised using the *Populus actin2* gene (*Potri.001G309500*). Primer pairs used for real-time PCR are as described previously (Gui *et al.*, 2019).

Determination of biomass growth

Trees were collected to measure biomass at the 2-month-old stage when grown in a phytotron. To minimise the potential transpiration impact of plant weight measurement, a stem was obtained by quickly stripping off the leaves and measuring the fresh weight within 2 min. Roots were collected and washed with water to remove soil and weighed after sucking surface water from the root. After measurement of the fresh weight, all plant fractions were dried in a forced-draft oven at 55°C for 48 h, followed by measurement of their dry weight.

Stem hydraulic conductance measurement

The hydraulic conductance of the stem xylem in 2-month-old *Populus* trees was measured using a high-pressure flow meter (HPFM, Dynamax) following the manufacturer's instructions. In brief, the same length of the aerial part of trees from top to bottom (about 25 cm) was collected by cutting and quickly inserting into water, and then fixing into the HPFM instrument adaptor. The conductivity and flow of water were measured using a quasi-steady-state flow meter. To minimise the potential impact of diurnal periodicity on hydraulic conductance, all measurements were taken between 10:00 AM and 3:00 PM in the phytotron in

which the trees were grown (with 60% relative humidity and 24°C constant temperature).

Histochemical staining and immunolocalisation

Phloroglucinol-HCl staining was performed as described previously (Gui *et al.*, 2011). In brief, sections were stained with 1% phloroglucinol (w/v) in 12% HCl for 5 min and immediately observed under a microscope (Olympus BX53). Toluidine blue staining of paraffin-embedded tissue was performed as described previously (Gui *et al.*, 2016). GUS staining was performed as described (Gui *et al.*, 2011). Free-hand cross-sections of stems were incubated with a staining solution (100 mM $NaPO_4$ (pH 7.0), 10 mM ethylene diamine tetraacetic acid (EDTA), 2 mM 5-bromo-4-chloro-3-indolyl-β-GlcA, 0.5 mM $K_4Fe(CN)_6$, 0.5mM $K_3Fe(CN)_6$, 0.2% Triton X-100, and 20% methanol) at 37°C. The reaction was stopped, and chlorophyll was extracted using 75% ethanol. For immunolocalisation, samples were fixed with acetone, paraffin-embedded and immunolocalised with GUS-specific antibodies, as described previously (Gui *et al.*, 2014).

Transmission electron microscopic observation of cell walls

Cell wall thickness was observed by transmission electron microscopy as described (Song *et al.*, 2010). In brief, the eight stem internodes were collected and cut into 1.5–2 mm lengths and soaked in fixation buffer (3% paraformaldehyde and 0.5% glutaraldehyde in 0.1 M PBS, pH 7.4) and further fixed with 0.5% osmic acid. Then, the tissues were dehydrated and embedded in LR white resin (Polysciences, Warrington, PA, USA). Ultrathin sections were staining with uranyl acetate and lead citrate, and observed under an electron microscope (H-7650; HITACHI, Kyoto, Japan) at 80 kV.

Lignin analyses

Xylem tissue of debarked stem from 2-month-old trees was collected and dried at 65°C. The dried tissue was ground to a fine powder by ball milling and used to prepare alcohol insoluble residues, according to Song *et al.* (2016). The pretreated cell wall residues were used to determine lignin content using the Klason procedure, as described (Gui *et al.*, 2011). For thioacidolysis and two-dimensional (2D) nuclear magnetic resonance (NMR), dried xylem tissue was ground to fine powders by ball milling and extracted sequentially using water and 80% (v/v) ethanol to obtain extractive-free cell wall residues (CWRs) (Tarmadi *et al.*, 2018). Analytical thioacidolysis on CWR samples was performed as described previously (Yamamura *et al.*, 2012) and the released lignin monomers were derivatised with *N,O*-bis(trimethylsilyl)acetamide and quantified using gas chromatography-mass spectrometry (GC-MS; QP-2010 Plus, Shimadzu, Kyoto, Japan) using 4,4′-ethylenebisphenol as an internal standard (Yue *et al.*, 2012). For 2D NMR analysis, CWRs were further ball-milled and digested with crude cellulase (Cellulysin; Calbiochem, La Jolla, CA, USA) to obtain lignin-enriched CWRs, as described previously (Tobimatsu *et al.*, 2013; Lam *et al.*, 2017). The lignin-enriched CWRs (*c.* 25 mg) were then dissolved in dimethylsulfoxide-d_6/pyridine-d_5 (4 : 1, v/v) and subjected to NMR analysis. NMR spectra were acquired on a Bruker Biospin Avance™ III 800US system (Bruker Biospin, Billerica, MA, USA) equipped with a cryogenically cooled 5-mm TCI gradient probe. Adiabatic 2D HSQC experiments were carried out using the standard implementation with parameters described in Mansfield *et al.* (2012). Data processing and volume integration analysis was conducted using Bruker TopSpin 3.1 software (Bruker Biospin) with procedures described previously (Lam *et al.*, 2017; Tarmadi *et al.*, 2018).

Measurement of mechanical strength

Fresh stems of 8-month-old *Populus* trees grown in a glasshouse were prepared for mechanical strength analysis. Mechanical properties of stem were measured by a three-point bending test using a mechanical testing machine (HY-0580, http://www.hengyiyiqi.com) according to (Xi *et al.*, 2017). Modulus of rupture (MOR) in bending was calculated according to Kern *et al.* (2005).

Cell wall saccharification analysis

Xylem cell wall saccharification assays were performed as described (VanAcker *et al.*, 2016). Samples were collected after 3, 6, 9, 12, 24, 36, 48 or 60 h incubation with appropriate cellulase and β-glucosidase and then the amount of glucose released was measured. Total glucan was determined using the dinitrosalicylic acid (DNS) method according to Liu *et al.* (2013). To calculate total tree stem sugar yield, the saccharification of glucose yield was also presented based on total biomass of each plant stem.

Results

Modification of lignin biosynthesis through constitutive and cell-type-specific manners resulted in different growth performance

In our previous study, lignin biosynthesis in *Populus* was persistently suppressed when LTF1 was modified to become a phosphorylation-null form ($LTF1^{AA}$) (Gui *et al.*, 2019). Under the control of a constitutive promoter (cauliflower mosaic virus 35S promoter, CaMV35S), lignin biosynthesis suppression (LS) by overexpressing $LTF1^{AA}$ (designated as *35S-LS*) caused severe growth defects. The transgenics displayed not only a retarded stature, shortened internodes and stem diameter, but also had short petiole length and small-sized leaves (Fig. S1a–g). The constitutive suppression of lignin biosynthesis through overexpressing phosphorylation-null *LTF1* ($LTF1^{AA}$) affected growth.

To investigate whether suppression of lignin biosynthesis in different cell types affects plant growth, we attempted to modify lignin biosynthesis under the control of vessel-specific or fibre-specific promoters. After examination of a number of cell-type-specific promoters, the promoter from *PdDUF579-9*

(*Potri.005G141300*), which is specifically expressed in xylem fibres (Song *et al.*, 2014), was used for fibre-specific modification. The *PdDUF579-9* promoter (designated *PdDUF579-9p*) was cloned and combined with a 35S minimal promoter to construct the *PdDUF579-9p-35Smini* synthetic promoter. When the synthetic promoter was fused to a β-glucuronidase (GUS) gene (*PdDUF579-9p-35Smini-GUS*) (Fig. S2a) and transformed into *Populus*, it displayed fibre-specific activity (Fig. S2b) For vessel-specific modification, a promoter fragment (2068 bp) from *Populus XYLEM CYSTEINE PROTEASE1* (*XCP1; Potri.004G207600*) (Funk *et al.*, 2002) was cloned and combined with a 35S minimal promoter to generate *PdXCP1p-35Smini* promoter (Fig. S2a). We confirmed that *PdXCP1p-35Smini* showed an activity specific for xylem vessels when it was fused with the GUS gene (*PdXCP1p-35Smini-GUS*) and transformed into *Populus* (Fig. S2c).

The cell-type-specific expression of *PdDUF579-9p-35Smini-GUS* and *PdXCP1P-35Smini-GUS* in *Populus* was further verified by immunolocalisation with GUS-specific antibodies. *PdDUF579-9P-35Smini-GUS* was specifically localised in fibre cells (Fig. S2d), while *PdXCP1P-35Smini-GUS* was specifically localised in vessel cells (Fig. S2e); this localisation was highly consistent with the GUS staining results (Fig. S2b,c). In addition, the localisation region of the two promoter activity was in agreement with the high expression of *DUF579-9* and *XCP1* in the developing xylem region (Fig. S2e,f), according to the information documented in the AspWood resource (Sundell *et al.*, 2017).

Then the two synthetic promoters were fused with $LTF1^{AA}$ to generate *PdDUF579-9p-35Smini-*$LTF1^{AA}$ and *PdXCP1p-35Smini-*$LTF1^{AA}$ constructs, which were transferred to *Populus*. Transgenic lines harbouring *PdXCP1p-35Smini-*$LTF1^{AA}$ were designated as *V-LS* and transgenic lines harbouring *PdDUF579-9p-35Smini-*$LTF1^{AA}$ were designated as *F-LS*. Thirty-five independent *F-LS* transgenic lines with similar morphologies were identified and two representative transgenic lines, *F-LS #12* and *F-LS #27* were clonally propagated for detailed characterisation. Meanwhile, 67 independent *V-LS* transgenic lines were generated that displayed dramatic morphological changes. Two representative transgenic lines, *V-LS #45* and *V-LS #51*, were clonally propagated and used for further characterisation. The transgenic lines were first grown in a phytotron for 2 months (Fig. 1a) and then moved into a glasshouse (Fig. 1b). Compared with the wild-type control, *F-LS* transgenics did not show any noticeable growth change. However, the *V-LS* transgenics displayed severe dwarfism, small and dark-green leaves, and more branching (Fig. 1a,b). Specifically, the *V-LS* transgenics were reduced by 50–65% in height, 35–40% in stem diameter, 60–65% in internode length and 60–70% in leaf size compared with the control (Fig. 1c,h). Consistently, stem biomass production was reduced by more than 50% in *V-LS* transgenics when compared with the control, whereas *F-LS* transgenics showed slight increases in both fresh and dry biomass production (Fig. S3a,d). In addition, leaf and root biomass were reduced substantially in the *V-LS* transgenics (Fig. S3b,c,e,f). Collectively, fibre-specific modification of lignin biosynthesis showed normal growth, while vessel-specific modification resulted in growth defects and biomass reduction.

Vessels and fibres in xylem constitute a system of long-distance water transportation and mechanical support to sustain plant growth (Boerjan *et al.*, 2003). To examine how the cell-type-specific modification of lignin biosynthesis in xylem affected system functions such as water transportation, the hydraulic conductance of the stem was measured using a high-pressure flow meter (HPFM) (Dynamax). The *V-LS* transgenics showed a 50% reduction of hydraulic conductance, but no change was detected in the *F-LS* transgenics (Fig. 1i). Meanwhile, the *35S-LS* transgenics showed a 55% reduction in stem hydraulic conductance (Fig. 1i). These results suggested that suppression of lignin biosynthesis in vessels affected stem water conductance and may be crucial for plant growth. In addition, we examined stem mechanical strength. A bending test showed the order of the stem bending force as: wild-type > *F-LS* > *V-LS* transgenics (Fig. S4a). Compared with the wild-type, the MOR displayed a reduction in the *F-LS* transgenics but no significant difference in the *V-LS* transgenics. This should be attributed to the smaller stem diameter in the *V-LS* transgenics (Fig. S4b). The data suggested that lignin deposition in xylem vessels and fibres may have different effects on water conductance and mechanical properties.

Both *V-LS* and *F-LS* transgenics showed a four- to six-fold increase in the *LTF1* transcripts (measurements included the *LTF1* and $LTF1^{AA}$ transcripts) compared with the control (Fig. 2a). Then, we measured the expression of secondary cell wall (SCW) biosynthesis-related genes (lignin biosynthesis genes: *4CL1*, *CAld5H*, *COMT2* and *CCoAOMT1*; cellulose biosynthesis genes: *CESA4*, *CESA7* and *CESA8*; and xylan biosynthesis genes: *GT43B* and *GT8D*). The transcript abundances of the key lignin biosynthesis genes *4CL1*, *COMT2* and *CCoAOMT1* were substantially suppressed in both *V-LS* and *F-LS* transgenics (Fig. 2a), while the transcript abundances of cellulose and xylan biosynthesis genes were not significantly suppressed, suggesting a specific suppression of lignin biosynthesis (Fig. 2b). Interestingly, transcript abundances of the lignin biosynthesis genes in developing xylem were less suppressed in the *V-LS* transgenics than in the *F-LS* transgenics (Fig. 2a). This difference may reflect the ratio of vessel and fibre cell populations in xylem tissue. The expression of *CAld5H*, which encodes a key enzyme for S-lignin biosynthesis (Meyer *et al.*, 1998; Osakabe *et al.*, 1999; Li *et al.*, 2003), was reduced in the *F-LS* transgenics but not in the *V-LS* transgenics (Fig. 2a). These results indicated that expression levels of lignin biosynthesis genes were differentially modified through fibre-specific or vessel-specific manners.

Different patterns of lignification and SCW formation observed in vessel and fibre cells

To examine SCWs in xylem, cross-sections of the stems at the 11th internode were dissected. In the *F-LS* transgenics, lignin deposition was reduced in fibre cell walls with no apparent changes in vessel walls as determined by lignin staining using phloroglucinol-HCl (Fig. 3a,c,d,f). By contrast, the *V-LS* transgenics developed thin-walled and deformed vessels and lignin

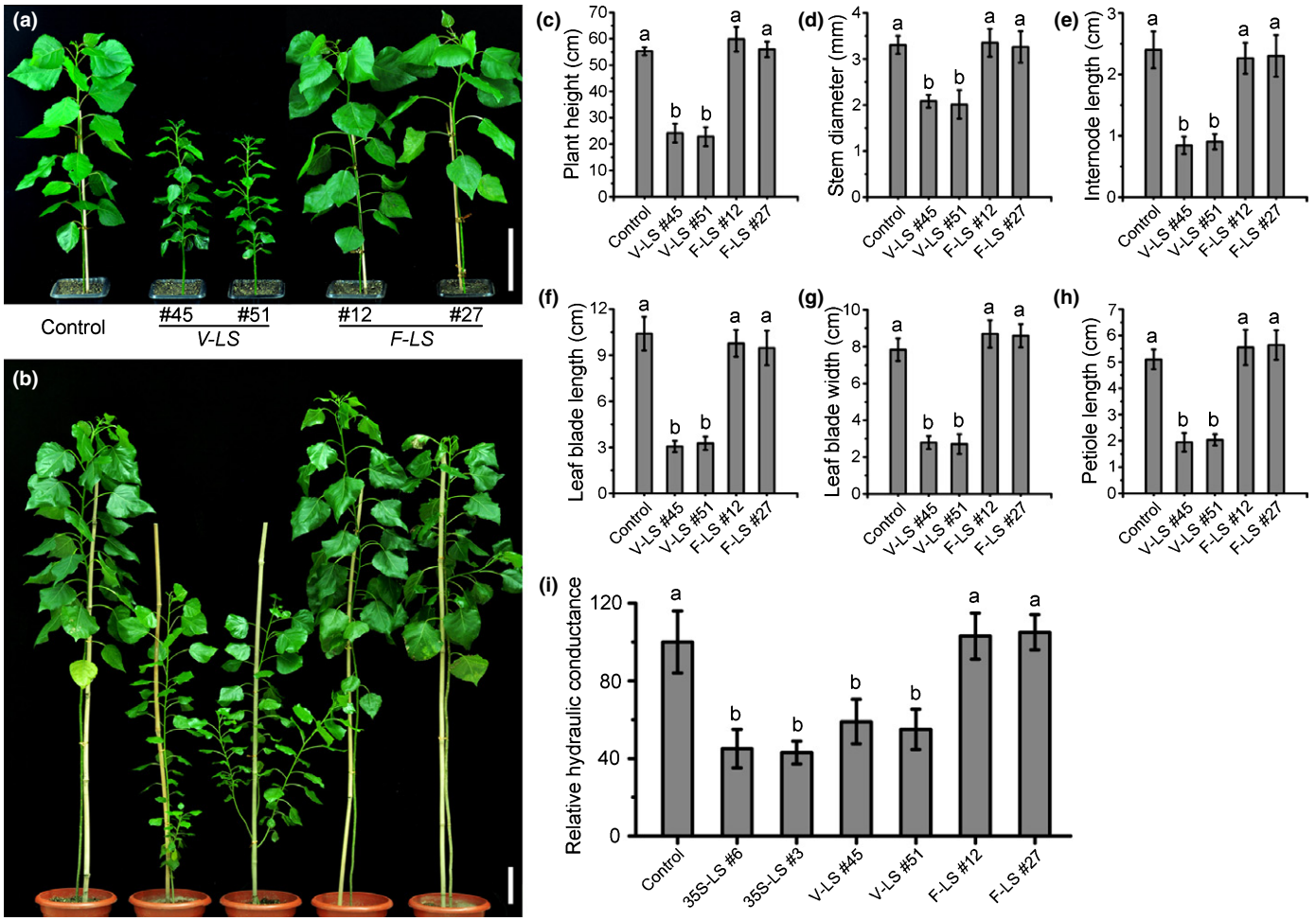

Fig. 1 Different phenotypes of the vessel-specific and fibre-specific overexpression of *LTF1*^{AA} in *Populus*. (a, b) Phenotypes of the *LTF1*^{AA} vessel-specific (*V-LS*) and fibre-specific (*F-LS*) overexpression plants grown in phytotron at 2 months old (a) and grown in glasshouse at 8 months old (b). Bars, 10 cm. (c–h) Plant height (c), stem diameter (d), internode length (e), leaf blade length (f), leaf blade width (g) and petiole length (h) of the transgenic and control plants were measured at 2 months old. Plant height and stem diameter: means ± SE of eight clonally propagated plants; the other parameters: means ± SE of 40 internodes from eight plants. (i) Relative hydraulic conductance was measured using a high-pressure flow meter. The hydraulic conductance in control plants was set at 100%. Relative hydraulic conductance: means ± SE of six clonally propagated plants. Different lowercase letters in (c–i) indicate significant differences at $P < 0.01$ by ANOVA.

deposition in fibre cell walls showed no change compared with the wild-type (Fig. 3a,b,d,e). In the *F-LS* transgenics, cells were well organised in xylem while, in the *V-LS* transgenics, xylem cells were disorganised with deformed vessels (Fig. 3g–i).

The SCW thickness in the *V-LS* transgenics was reduced by 40–50% in vessels with no change in fibres (Fig. 3j,k,m,n). By contrast, the *F-LS* transgenics showed no change in SCW thickness in vessels but the SCW thickness was reduced by 35–45% in fibres (Fig. 3j,l–n). These results indicated that lignification and SCW formation were modified in vessels and fibres in a cell-type-specific manner. In comparison, we also examined xylem cells in the *35S-LS* transgenics. The *35S-LS* transgenics displayed distorted and collapsed vessel cells and larger but less lignified fibre cells (Fig. S5a,b). Both vessels and fibres were modified to thinner SCWs (Fig. S5c,d). The SCW thickness was substantially decreased (Fig. S5e,f) by 40% and 45% in xylem vessels and fibres, respectively (Fig. S5g,h). In addition, the majority of the vessels in the *35S-LS* transgenics displayed a wall-deformed structure (Fig. S5i). Constitutive suppression of lignin biosynthesis resulted in defective SCW of both vessels and fibre cells in xylem.

Lignin abundance and composition was modified in a cell-type-dependent manner

Lignin deposition was modified in the vessels of the *V-LS* transgenics and in the fibres of the *F-LS* transgenics. Lignin content and monolignol composition of CWR samples prepared from the control and transgenic xylem tissues were measured using the Klason and thioacidolysis methods, respectively. The Klason lignin content was reduced by 43% in the *F-LS* transgenics and by 16% in the *V-LS* transgenics (Table 1). Meanwhile, lignin in the *35S-LS* transgenics was more drastically reduced by 56% (Table 1); this might reflect the lignin modification in both vessels and fibres. The *F-LS* transgenics with the lignin reduction by 43% did not show any apparent growth defects (Fig. 1a,b). However, the *V-LS* transgenics displayed, similarly to the *35S-LS*, serious growth defects

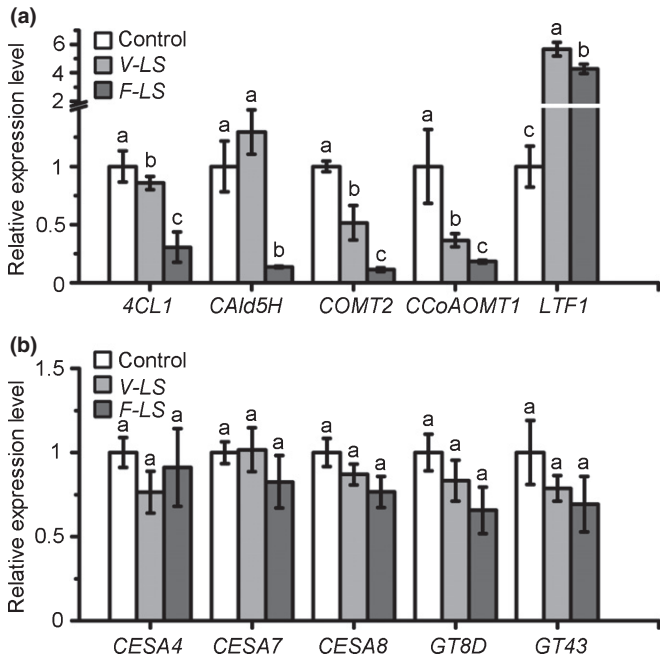

Fig. 2 Expression of secondary cell wall biosynthesis genes in the transgenic and control plants. (a) Lignin biosynthesis genes. (b) Cellulose and hemicellulose biosynthesis genes. The developing xylem tissues of the 2-month-old plants were used to examine gene expression using quantitative RT-PCR (qRT-PCR) analysis. The *Populus actin2* gene was used as a reference for normalisation. Gene expression in the control was set as 1. Results are the means ± SE of three biological replicates. The same lowercase letter indicates that there is no significant difference at $P < 0.01$ by ANOVA.

(Figs 1, S1), although the lignin content in the *V-LS* transgenics was more mildly reduced by 16%. This result suggests that cell-type-specific lignin deposition plays a critical role in plant growth.

Analytical thioacidolysis, which releases quantifiable H-, G-, and S-type monomeric degradation products via cleavage of β–*O*–4 linkages in lignin polymers (Lapierre *et al.*, 1986), determined substantially altered lignin subunit composition and S : G ratio in the three kinds of the transgenic lines. Consistent with the Klason lignin content data (Table 1), the total yields of the lignin-derived monomeric products released from the three transgenic lines were all reduced compared with that determined for the wild-type control. The lignin-derived monomeric products were principally composed of G- and S-types with much lower amounts of H-type (about 0.2–0.6%). Our data suggested that G- and S-type products were disproportionately reduced in the three transgenic lines. For the *V-LS* transgenics, G-type products were reduced by 18% and S-type products by 9%, leading to an increase in the S : G ratio. For the *F-LS* transgenics, conversely, G-type products were reduced by 31% and S-type products by 52%, resulting in a decrease in the S : G ratio. Given that vessel and fibre cell walls in typical dicot species are relatively enriched in G- and S-lignin units, respectively (Boerjan *et al.*, 2003; Nakashima *et al.*, 2008), such increase and decrease of the S : G ratio in the *V-LS* and *F-LS* lines are in line with our idea that their lignin reduction is cell type specific for vessels and fibres, respectively (Fig. 3a–f). For the *35S-LS* transgenics, G-type products were reduced by 37% and S-type products by 78%. The larger reduction in S-type products may reflect a higher percentage of fibres than vessels in xylem. Overall, our data suggest that the majority of lignin in xylem is from fibres, in which suppression of lignin biosynthesis primarily caused a reduction in S units, but suppression of lignin biosynthesis in vessels was mostly related to G-unit reduction.

To further examine lignin composition and structure, we performed solution-state two-dimensional (2D) nuclear magnetic resonance spectroscopy (NMR) analysis on lignin-enriched CWR samples prepared via enzymatic removal of cell wall polysaccharides. The aromatic subregions of the short range $^{1}H–^{13}C$ correlation (HSQC) spectra displayed contour signals from G and S aromatic units along with those from *p*-hydroxybenzoates (*p*Bz) acylating a fraction of poplar lignin (Venverloo, 1971; Morreel *et al.*, 2004; Stewart *et al.*, 2009) and cinnamyl alcohol end-groups (X_1) (Fig. 4). Volume integration of $C_2–H_2$ signals from G and S units suggested that the S : G ratio was increased in the *V-LS* transgenics (S : G, 1.2), but decreased in the *F-LS* (S : G, 0.7) and *35S-LS* (S : G, 0.3) transgenics, compared with the control (S : G, 1.0) (Fig. 4). The change in the S : G ratio in each transgenic line is overall in line with the results of thioacidolysis, as described above (Table 1). In addition, we observed that the relative intensity of *p*Bz signals was increased in the spectrum of the *V-LS* lignin, but reduced in the spectra of the *F-LS* and *35S-LS* lignins. As *p*-benzoate preferentially acylates S units over G units in typical poplar lignin (Stewart *et al.*, 2009), the data further corroborate the shifts of S : G ratio in the three transgenic lines.

The aliphatic subregions of the HSQC spectra display countersignals from the major intermonomeric linkages, such as β-aryl ether (β–*O*–4, I), phenylcoumaran (β–5, II), resinol (β–β, III) and spirodienone (β–1, IV), in the lignin polymer. Volume integration of $C_\alpha–H_\alpha$ signals suggested that the *V-LS* transgenics had proportionally decreased β–5 units, whereas *F-LS* and *35S-LS* had conversely increased β–5 units (Fig. 5). Because β–5 linkages can be only formed in G units derived from the polymerisation of coniferyl alcohol, the increase in β–5 units is consistent with the decreased S : G ratios in the *35S-LS* and *F-LS* transgenics and in agreement with previous studies on transgenic plants with altered S : G ratios (Stewart *et al.*, 2009; Anderson *et al.*, 2015; Takeda *et al.*, 2017; Takeda *et al.*, 2019). Taken together, both thioacidolysis and 2D NMR data support our idea that G-rich vessel and S-rich fibre lignins are precisely altered in the transgenics obtained in this study.

Fibre-specific suppression of lignin biosynthesis improved biomass quality and sustained vigorous growth in field

As the *F-LS* and *V-LS* transgenic *Populus* displayed different growth under laboratory conditions, we further evaluated their growth performance in field. The transgenic trees were grown in a field in Shanghai (Crop Cultivation and Breeding Station, SIPPE, China) for a full growth season. *F-LS* transgenics showed a similar growth performance with the control trees in height, stem diameter and aboveground biomass (Fig. 6a,b). However,

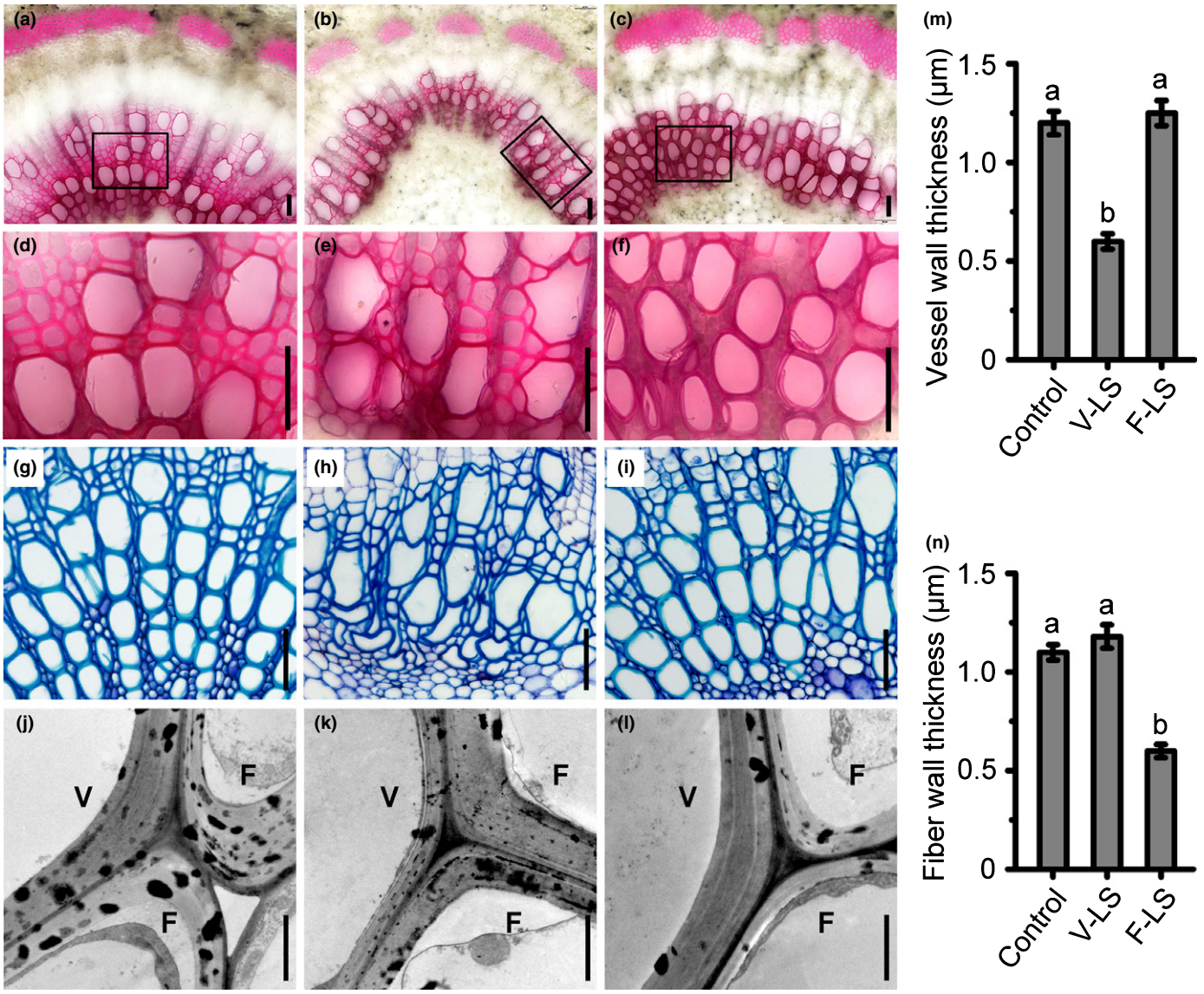

Fig. 3 Vessel-specific and fibre-specific overexpression of *LTF1*^{AA} resulted in reduction of lignin biosynthesis and cell wall thickness in vessels and fibres, respectively. (a–f) Cross-sections (11th internode) of the control (a), *V-LS* (b) and *F-LS* (c) stained for lignin using phloroglucinol-HCl. Close-up images of the control (d), *V-LS* (e) and *F-LS* (f) indicated with rectangle in (a–c). Bars, 50 μm. (g–i) Paraffin-embedded sections (11th internode) of the control (g), *V-LS* (h) and *F-LS* (i) stained with toluidine blue. Bars, 50 μm. (j–l) Transmission electron micrographs display xylem fibre and vessel cell wall in the control (j), *V-LS* (k) and *F-LS* (l) transgenics. F, fibre cell; V, vessel cell. Bars, 2 μm. (m, n) Cell wall thickness in the vessels (m) and fibres (n) from control, *V-LS* and *F-LS* transgenics. In control, *V-LS* and *F-LS* transgenics, 20 vessel cells and fibre cells from each of four independent plants were measured. Different lowercase letters in (m) and (n) indicate significant differences at $P < 0.01$ by ANOVA.

V-LS transgenics displayed retarded growth with reduction in height, stem diameter and aboveground biomass (Fig. 6a,b). More specifically, plant height was reduced by 56–63%, stem diameter by 39–48%, and aboveground biomass by 75–89% in the *V-LS* transgenics compared with the control (Fig. 6c,e). These results showed that fibre-specific modification of lignin biosynthesis maintained vigorous growth in fields, whereas vessel-specific modification resulted in a growth penalty with biomass reduction. We further observed cell morphology and lignin staining of xylem tissues of the field-grown trees. The *V-LS* transgenics contained deformed or collapsed vessels with regular and normally lignified fibre cell walls (Figs 6f,g, S6a,b,d,e,g,h). By contrast, *F-LS* transgenics contained less lignin in fibre cell walls, but lignin deposition was normal in vessel walls (Figs 6f,h, S6a,c, d,f,g,i). Lignin modification in specific cell types, therefore, differentially affected field growth performance.

In addition, we carried out saccharification analysis using wood stem materials. The *35S-LS* and *F-LS* transgenics showed a higher efficiency of glucose release than the *V-LS* transgenics (Fig. 6i). After 60 h of enzyme digestion, glucose release from the *35S-LS* and *F-LS* wood material was increased by 70% and 45%, respectively, compared with the control, whereas glucose release from the *V-LS* material was not significantly different from the control (Fig. 6i). It is likely that the more drastic lignin reductions in *35S-LS* and *F-LS* wood materials contributed to the improved saccharification efficiency. Although

Table 1 Determination of lignin content and monolignol composition in *LTF1*^{AA} transgenic plants.

Sample	Klason lignin (% CWR)	Thioacidolysis-derived monomer composition (μmol g^{-1} CWR)				Thioacidolysis-derived monomer reduction (%)		
		H	G	S	Total H + G + S	G	S	S : G ratio
Control	22.18 ± 0.63^{a}	1.64 ± 0.14	293.62 ± 23.43	354.09 ± 57.22	649.34 ± 63.99^{a}	-	-	1.21 ± 0.20^{b}
35S-LS	9.85 ± 0.51^{d}	1.80 ± 0.15	184.58 ± 28.13	76.34 ± 13.57	262.71 ± 41.80^{d}	37^{a}	78^{a}	0.41 ± 0.01^{d}
V-LS	18.56 ± 0.73^{b}	1.06 ± 0.03	238.77 ± 12.90	320.06 ± 15.34	559.88 ± 28.19^{b}	18^{b}	9^{c}	1.34 ± 0.01^{a}
F-LS	12.54 ± 0.41^{c}	1.50 ± 0.06	202.39 ± 18.38	168.82 ± 19.52	372.72 ± 37.31^{c}	31^{a}	52^{b}	0.83 ± 0.04^{c}

Results are means ± SE of three biological replicates. Different lowercase letters indicate that the difference of Klason lignin content or total thioacidolysis monomer yield between the control and transgenic trees is statistically significant at $P < 0.01$ by ANOVA.

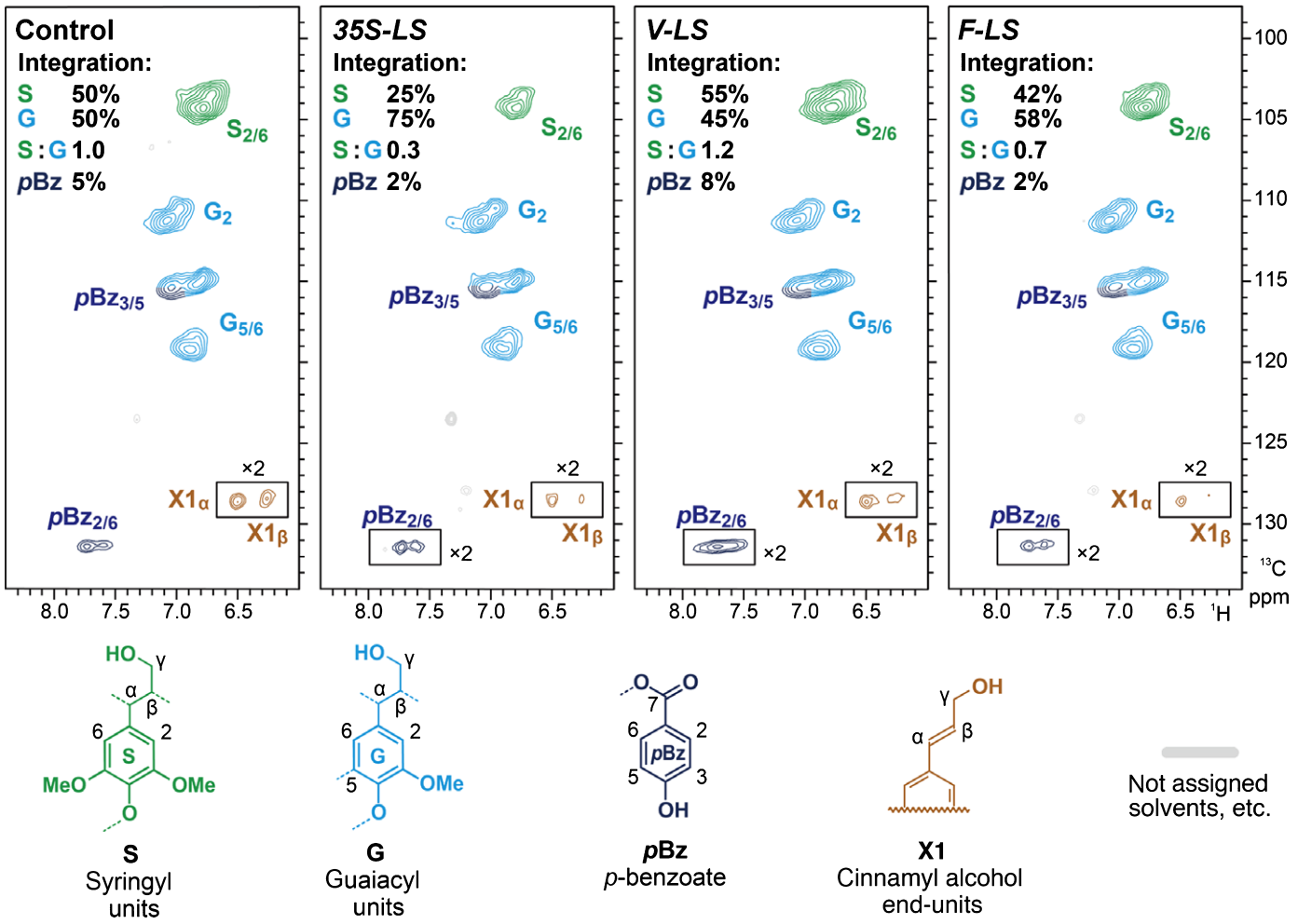

Fig. 4 Aromatic subregions of short range ^{1}H–^{13}C correlation (HSQC) NMR spectra of lignin from xylem tissue. The 2D NMR spectra of lignin samples prepared from the control, constitutive (*35S-LS*), vessel-specific (*V-LS*) and fibre-specific (*F-LS*) overexpression of *LTF1*^{AA} in *Populus* are shown. Volume integrals are given for the aromatic units that are colour coded to match their assignments in the spectra. The percentages noted in each spectrum are integrals expressed relative to the total S + G aromatic units. Boxes labelled × 2 indicate regions that are vertically scaled up by two-fold.

saccharification efficiency was increased in *35S-LS* lines, the total glucose yield per plant was significantly reduced due to the dramatic decrease in biomass yield. As shown in Fig. 6(j), the relative glucose yield per plant reflected a combination of saccharification efficiency, glucan content and plant biomass yield. The *F-LS* transgenics displayed a relative increase of glucose yield per plant by 67% compared with the control. By contrast, glucose yield per plant was decreased by 65% with *35S-LS* transgenics and by 60% with *V-LS* transgenics. These results indicated that lignin modification through a fibre-specific manner can be applicable for improvement of wood biomass production without growth penalty.

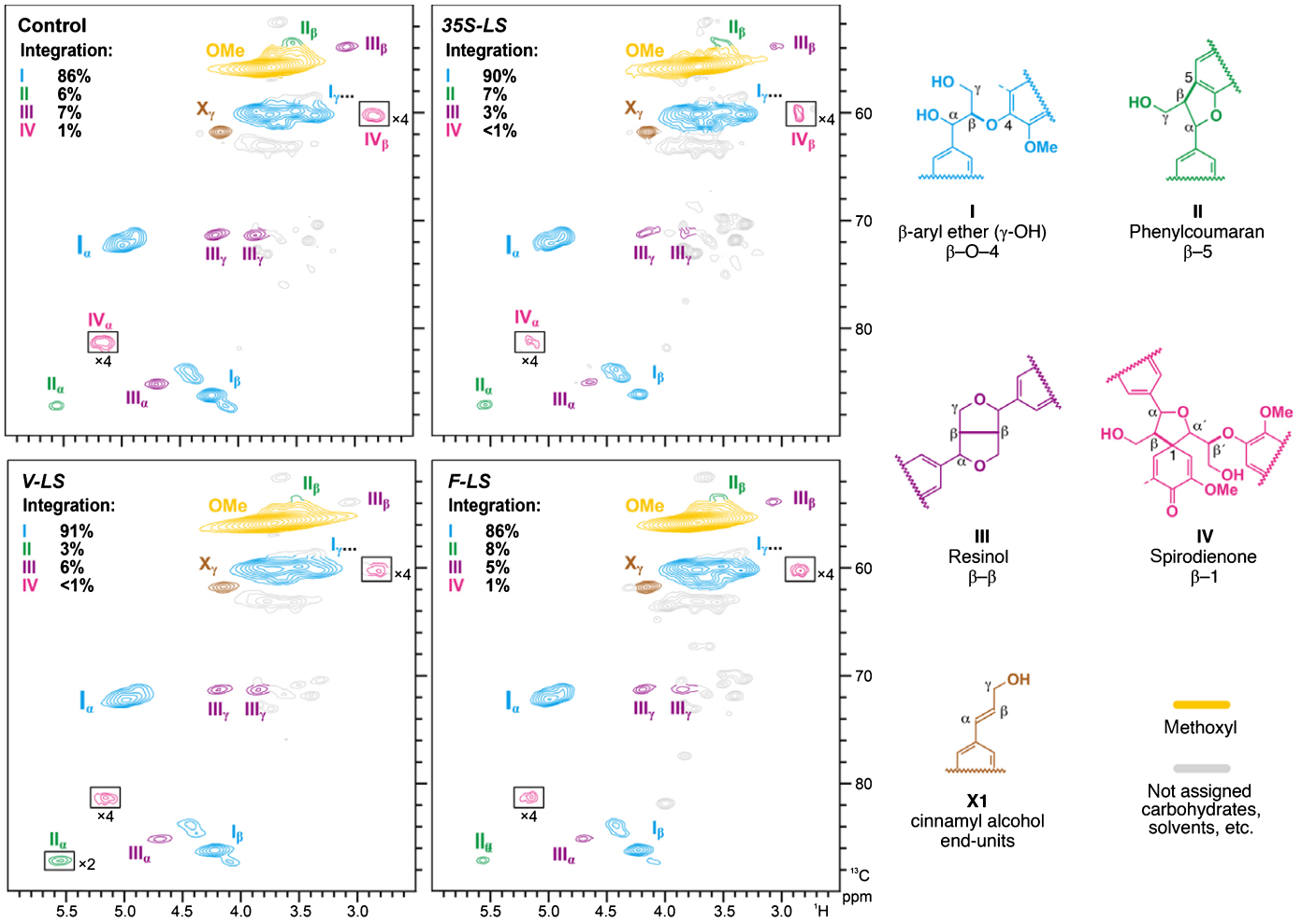

Fig. 5 Aliphatic subregions of short range ^{1}H–^{13}C correlation (HSQC) NMR spectra of lignin from xylem tissue. The 2D NMR spectra of lignin samples prepared from the control, constitutive (*35S-LS*), vessel-specific (*V-LS*) and fibre-specific (*F-LS*) overexpression of $LTF1^{AA}$ in *Populus* are shown. Volume integrals are given for the major lignin side-chain structures that are colour-coded to match their assignments in the spectra. The percentages noted in each spectrum are integrals expressed relative to the total I, II, III and IV side-chain structures. Boxes labelled × 2 and × 4 indicate regions that are vertically scaled up by two-fold and four-fold, respectively.

Discussion

Lignin biosynthesis in different cell types plays distinct roles in growth

Lignin is synthesised specifically in the SCWs of vascular plants, fortifying the mechanical strength of walls and providing wall hydrophobicity for long-distance transportation of water (Weng & Chapple, 2010). During xylem differentiation in angiosperms, lignin is synthesised in fibre and vessel cells. Much evidence has accumulated to elucidate lignin biosynthesis in plants (Boerjan *et al.*, 2003; Barros *et al.*, 2015; Meents *et al.*, 2018; Vanholme *et al.*, 2019). However, the role of lignin biosynthesis in different cell types is not fully understood.

In this study, we employed a lignin-related transcription factor gene *LTF1*, which had been modified to convey persistent suppression of lignin biosynthesis (Gui *et al.*, 2019). The engineered *LTF1* ($LTF1^{AA}$) allowed us to obstruct lignin biosynthesis in specific types of cells under the control of cell-type-specific promoters. Constitutive expression of $LTF1^{AA}$ (*35S-LS*) suppressed lignin biosynthesis in xylem tissue with development of defective SCWs in both xylem vessels and fibres, resulting in severe growth defects with retarded stature, shortened internodes, stem diameter and petiole length, and the small-sized leaves of the *35S-LS* transgenic trees (Fig. 7). When lignin biosynthesis was suppressed by overexpression of $LTF1^{AA}$ in vessels (*V-LS*), the transgenic trees developed defective SCWs in vessel and displayed a similar growth as the found for *35S-LS* (Fig. 7). However when lignin biosynthesis was suppressed by overexpression of $LTF1^{AA}$ in fibres (*F-LS*), the *F-LS* transgenic trees contained effective vessels and grew normally (Fig. 7). These results suggested that lignin biosynthesis in different cell types plays distinct roles in plant growth.

Disruptions to lignin biosynthesis often causes abnormal lignin deposition in lignified cells, such as xylem vessels, fibres and other cells, and can lead to abnormal plant growth and development including dwarfed morphology and defects in fertility (Leple *et al.*, 2007; Shadle *et al.*, 2007; Yang *et al.*, 2007; Nakashima

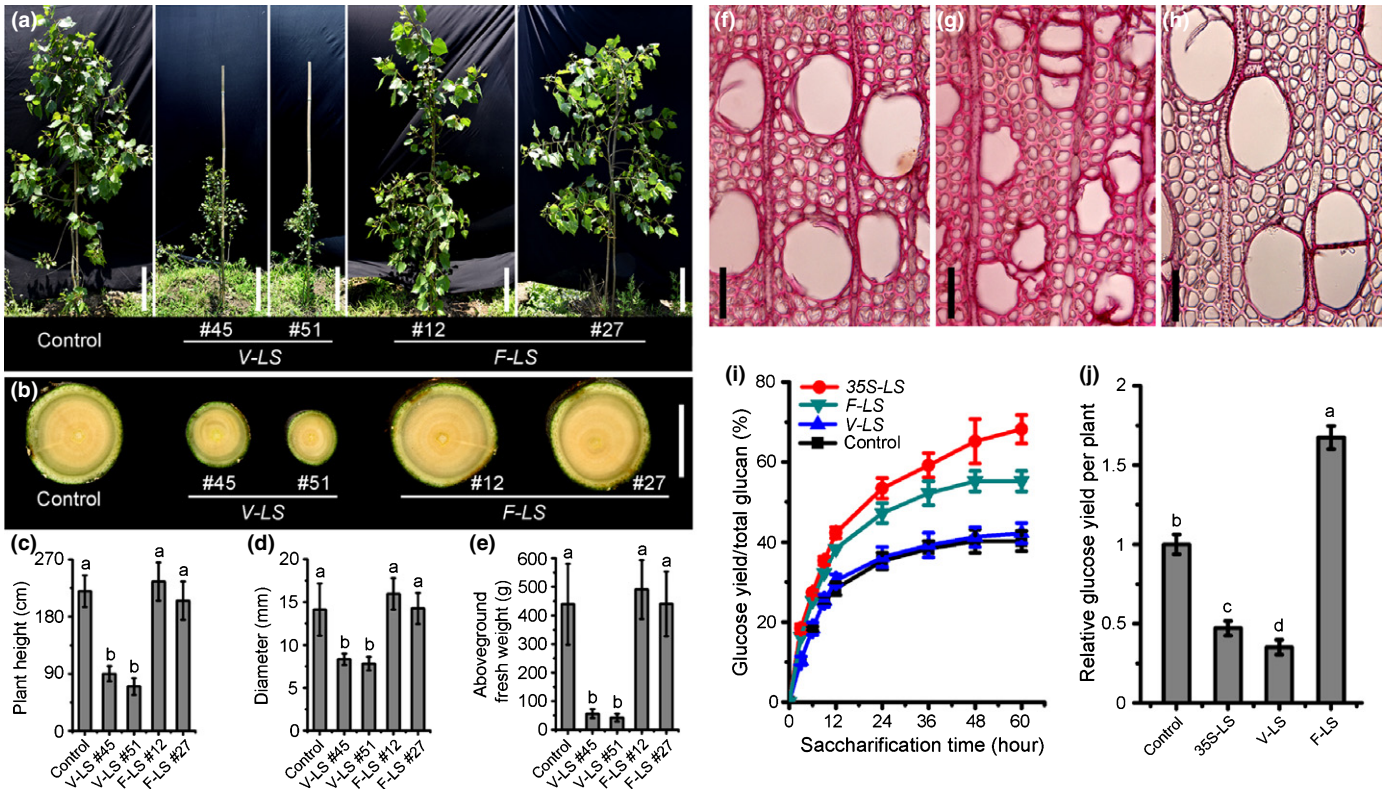

Fig. 6 Phenotypes of the vessel-specific and fibre-specific overexpression of *LTF1*^{AA} were grown in field condition. (a) Morphology of the 1-yr-old *LTF1*^{AA} vessel-specific (*V-LS*) and fibre-specific (*F-LS*) overexpression trees grown in field condition. Bars, 30 cm. (b) Stem base transverse sections of the control, *V-LS* and *F-LS* transgenic trees. Bar, 1 cm. (c–e) Field-grown plant height (c), stem diameter (d), and aboveground fresh weight (e) of the transgenic and control plants were measured at 1-yr-old. Plant height, diameter and aboveground fresh weight: means ± SE of six clonally propagated plants. (f–h) The stem base cross-sections (14 μm thick) of the control (f), *V-LS* (g) and *F-LS* (h) were stained with phloroglucinol-HCl. Bars, 50 μm. (i) Saccharification efficiency of stem biomass. Glucose yield was measured at 3, 6, 9, 12, 24, 36, 48 or 60 h after saccharification. Saccharification efficiency is expressed as the percentage of total glucan. (j) Relative glucose yield based on each plant. The glucose yield in the control plant after 60 h saccharification is set as 1. The values represent means ± SE of three biological replicates. Different lowercase letters in (c–e) indicate significant differences at $P < 0.01$ by ANOVA.

et al., 2008; Voelker *et al.*, 2010; Gui *et al.*, 2011; Van Acker *et al.*, 2014). For example, lignin biosynthesis in endothecium cells is required for anther dehiscence and pollen release for pollination (Yang *et al.*, 2007). Pod shatter also requires specific lignification of the valve margin cells to create tension for valve separation from the replum (Liljegren *et al.*, 2000).

Modification of lignin biosynthesis in various type cells can disrupt proper cell function (Barros *et al.*, 2015). Evidence showed that, for example, whereas mutations of lignin biosynthetic enzyme genes such as *cinnamic acid 4-hydroxylase* (*C4H*) (Schilmiller *et al.*, 2009), *cinnamoyl coenzyme A reductase* (*CCR*) (Jones *et al.*, 2001) and *caffeoyl shikimate esterase* (*CSE*) (Vanholme *et al.*, 2013) in Arabidopsis resulted in abnormal lignin biosynthesis, vessel cell wall defects and slow growth, particular restoration of these enzyme functions in vessels helped to rebuild vessel integrity and growth performance (Yang *et al.*, 2013; Vargas *et al.*, 2016; De Meester *et al.*, 2018). In addition, incorporation of unconventional monolignols into lignin polymers via lignin engineering improved biomass digestibility without growth penalty in *Populus* (Wilkerson *et al.*, 2014; Cai *et al.*, 2016).

In this study, hydraulic conductance in the stem of transgenic plants was reduced after the repression of lignin biosynthesis in vessels, while fibre-specific suppression of lignin biosynthesis did not affect hydraulic conductance. Therefore, our data demonstrate that lignin deposition in xylem vessels is required for vessel function in long-distance transportation of water that in turn is essential for plant normal development and growth.

Distinctive lignin compositions in vessels and fibres

In the cell-type specifically modified *Populus*, lignin content and lignin monomers composition were changed greatly. Lignin content was reduced by 56%, 43% and 16%, respectively, in the xylem tissue of *35S-LS*, *F-LS* and *V-LS* transgenics (Table 1). The reduction of lignin content reflected lignin biosynthesis, which was suppressed in both vessels and fibres under the control of a *CaMV 35S* promoter (*35S-LS*), in fibres under the control by a fibre-specific promoter (*F-LS*), and in vessels under the control of a vessel-specific promoter (*V-LS*). In *Populus*, there is a higher proportion of xylem fibres than vessels in secondary xylem tissue (Takata *et al.*, 2019); this could explain why suppression of lignin biosynthesis in fibres resulted in larger lignin reduction than that in vessels (Table 1).

It is believed that lignin monomer composition varies among cell types. The current understanding of cell-type-specific lignin composition is primarily based on evidence provided by

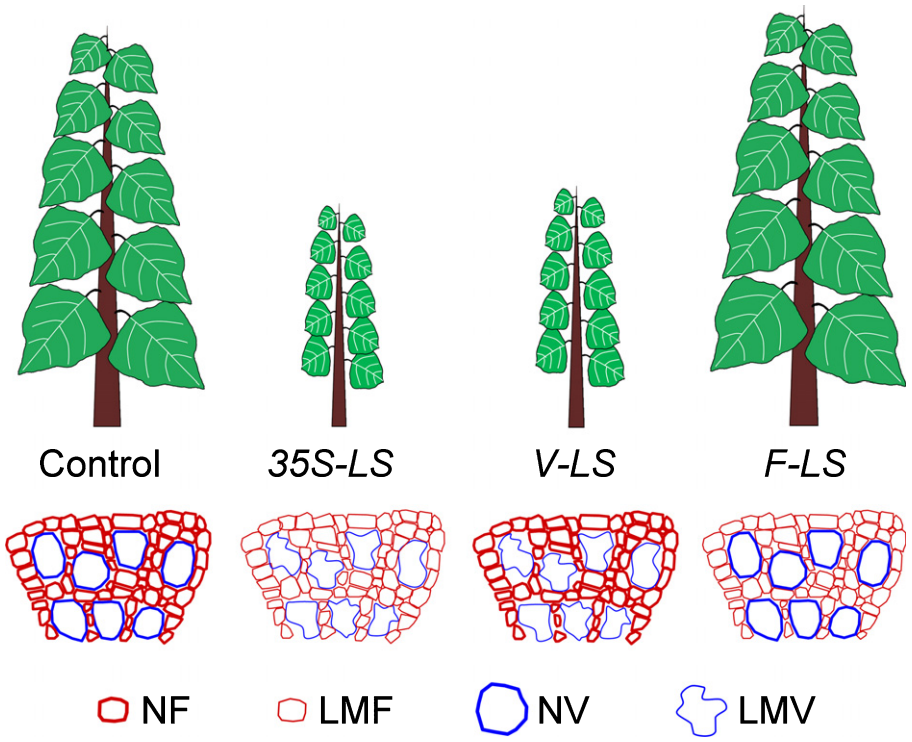

Fig. 7 A schematic illustration of lignin biosynthesis modification in different types of cells in *Populus*. *LTF1*^{AA}, a persistent repressor of lignin biosynthesis, was introduced into *Populus* under the control of a vessel-specific (*XCP1P*) or a fibre-specific (*DUF579-9P*) promoter to suppress lignin biosynthesis in a cell-type-specific manner. Indiscriminate suppression of lignin biosynthesis by constitutive expression of *LTF1*^{AA} (*35S-LS*) leads to severe dwarfism and development of defective secondary cell walls (SCWs) in both vessels and fibres. The trees with lignin suppression in vessels (*V-LS*) showed severe dwarfism and defective SCWs in vessels but normal SCWs in fibres. The trees with lignin suppression in fibres (*F-LS*) displayed vigorous growth with normal SCWs in vessels and thinner SCWs in fibres. LMF, lignin-modified fibres; LMV, lignin-modified vessels; NF, normal fibres; NV, normal vessels.

ultraviolet (UV) light microscopy, FT-IR microspectroscopy or X-ray analysis (Saka *et al.*, 1988; Foster *et al.*, 2010; Gorzsas *et al.*, 2011). However, more precise determination of lignin monomer composition in different cell types still remains to be addressed. The specific suppression of lignin biosynthesis in different types of cells in the secondary xylem tissue, and examination of the expression of lignin biosynthetic genes and the lignin composition in the transgenics illustrated a quantification of lignin monomers in fibres and vessels. Interestingly, *CAld5H*, the key enzyme for S-lignin biosynthesis (Meyer *et al.*, 1998; Osakabe *et al.*, 1999; Li *et al.*, 2003), was not suppressed in the *V-LS* transgenics, but significantly suppressed in the *F-LS* transgenics, suggesting that S-lignin biosynthesis may take place primarily in fibre cells. This idea was further verified by thioacidolysis and 2D NMR analyses. Suppression of vessel lignin biosynthesis resulted in more G-unit reduction, whereas suppression of fibre lignin biosynthesis conversely resulted in more S-unit reduction (Table 1; Fig. 4). In line with these observations, 2D NMR further revealed that phenylcoumaran (β–5) linkages unique in G-lignin units were proportionally reduced in the transgenics of vessel-specific lignin suppression (*V-LS*) whereas the transgenics of fibre-specific lignin suppression (*F-LS*) produced lignin with more β–5 units. These results provided a line of quantitative evidence suggesting that, in xylem tissue vessel, cells are enriched in G-lignin while fibre cells are predominantly composed of S-lignin.

Suppression of lignin biosynthesis in xylem fibres improves biomass production without penalising plant growth

Lignin plays various roles in different cell types for plant growth and development. Meanwhile, lignin is also a limiting factor in utilisation of the most abundant and renewable lignocellulosic biomass for production of fibre materials and biofuels (Chen & Dixon, 2007; Vanholme *et al.*, 2013; Van Acker *et al.*, 2014). To overcome this lignin barrier in biomass deconstructions, a great deal of interest has been invested in modification of lignin biosynthesis through manipulating key genes encoding the pathway enzymes and transcription factors involved in lignin biosynthesis. For example, reduction in lignin content has been achieved by downregulation of *4-coumarate:coenzyme A ligase* (*4CL*) in poplar (Hu *et al.*, 1998; Voelker *et al.*, 2010), *caffeic acid O-methyltransferase* (*COMT*) in switchgrass (Fu *et al.*, 2011), *4-coumarate 3-hydroxylase* (*C3H*) and *hydroxycinnamoyl CoA: shikimate hydroxycinnamoyl transferase* (*HCT*) in alfalfa (Shadle *et al.*, 2007). In addition, combinational modification of multiple lignin biosynthesis genes to alter lignin monomer composition and content were achieved in poplar and rice (Li *et al.*, 2003; Gui *et al.*, 2011).

Although the strategies to modify lignin biosynthesis genes to reduce lignin content and increase biomass saccharification efficiency have significant potential for biotechnology applications, traditional strategies for lignin reduction through a constitutive

or a tissue-specific manner often cause stunted growth and reductions in biomass yield that impose considerable limitations on their application. To optimise the benefit from lignin modification, we carried out a precise regulation of lignin biosynthesis in specific cell types using LTF1, a transcription factor. LTF1 is able to modulate expression of the multiple key genes in the lignin biosynthesis pathway and regulate the entire metabolic flux to lignin deposition (Gui *et al.*, 2019). In addition, the engineered LTF1 ($LTF1^{AA}$) is more stable and can provide a persistent suppression of lignin biosynthesis. Suppression of lignin biosynthesis in fibre cells improved biomass production without growth defects, whereas suppression of lignin biosynthesis in vessel cells caused growth defects and substantial reduction in biomass yield.

Lignin suppression in different cell types showed different growth performance, biomass yield and glucose yield through saccharification. Based on our analysis, the glucose yield after saccharification was increased by 67% in the transgenics with fibre-specific suppression of lignin biosynthesis, while the transgenics with vessel-specific suppression of lignin biosynthesis showed a 65% reduction in glucose yield. Modification of lignin in fibres displayed a significant potential to reduce cell wall recalcitrance in biomass conversion, as well as improve biomass production without growth penalty. Next, a larger scale of field test would be necessary to evaluate the applicability of this approach of lignin engineering. Nevertheless, this study opens an avenue to more precisely manipulate lignin deposition and improve lignocellulosic biomass property and production.

Acknowledgements

We thank Xiaoyan Gao, Jiqin Li and Zhiping Zhang for their support in transmission electron microscopy and Hironori Kaji and Ayaka Maeno for their support in NMR experiments. Part of this study was conducted using the facilities in the DASH/FBAS at RISH and the NMR spectrometer in the JURC at ICR, Kyoto University. This work was supported by the National Natural Science Foundation of China (grant no. 31630014), Chinese Ministry of Agriculture (grant no. 2018ZX08020002), the Chinese Academy of Sciences (grant no. XDB27020104), the Youth Innovation Promotion Association CAS (grant no. 2017318), the Chinese Ministry of Science and Technology (grant no. 2016YFD0600104), the Japan Society for the Promotion of Science (JSPS; grant nos. 16K14958, 16H06198 and 17F17103), RISH, Kyoto University (Mission-linked Research Funding, no. 2016-5-2-1), and the China/Japan Scientific Cooperation Programme by NSFC/JSPS.

Author contributions

JG, TU and LL designed the research; JG, PYL, YT, JS, CH, SC, YZ performed the research. JG, PYL, YT, TU and LL analysed the data and wrote the manuscript.

ORCID

Jinshan Gui https://orcid.org/0000-0002-3298-5786
Laigeng Li https://orcid.org/0000-0001-6924-4431
Yuki Tobimatsu https://orcid.org/0000-0002-7578-7392
Toshiaki Umezawa https://orcid.org/0000-0003-1135-5387

References

Anderson NA, Tobimatsu Y, Ciesielski PN, Ximenes E, Ralph J, Donohoe BS, Ladisch M, Chapple C. 2015. Manipulation of guaiacyl and syringyl monomer biosynthesis in an Arabidopsis cinnamyl alcohol dehydrogenase mutant results in atypical lignin biosynthesis and modified cell wall structure. *The Plant Cell* **27**: 2195–2209.

Barros J, Serk H, Granlund I, Pesquet E. 2015. The cell biology of lignification in higher plants. *Annals of Botany* **115**: 1053–1074.

Benfey PN, Chua NH. 1990. The Cauliflower mosaic virus 35S promoter: combinatorial regulation of transcription in plants. *Science* **250**: 959–966.

Boerjan W, Ralph J, Baucher M. 2003. Lignin biosynthesis. *Annual Review of Plant Biology* **54**: 519–546.

Bonawitz ND, Kim JI, Tobimatsu Y, Ciesielski PN, Anderson NA, Ximenes E, Maeda J, Ralph J, Donohoe BS, Ladisch M *et al.* 2014. Disruption of mediator rescues the stunted growth of a lignin-deficient Arabidopsis mutant. *Nature* **509**: 376–380.

Cai Y, Zhang K, Kim H, Hou G, Zhang X, Yang H, Feng H, Miller L, Ralph J, Liu CJ. 2016. Enhancing digestibility and ethanol yield of *Populus* wood via expression of an engineered monolignol 4-*O*-methyltransferase. *Nature Communications* **7**: 11989.

Chen F, Dixon RA. 2007. Lignin modification improves fermentable sugar yields for biofuel production. *Nature Biotechnology* **25**: 759–761.

De Meester B, de Vries L, Ozparpucu M, Gierlinger N, Corneillie S, Pallidis A, Goeminne G, Morreel K, De Bruyne M, De Rycke R *et al.* 2018. Vessel-specific reintroduction of CINNAMOYL-COA REDUCTASE1 (CCR1) in dwarfed ccr1 mutants restores vessel and xylary fibre integrity and increases biomass. *Plant Physiology* **176**: 611–633.

Eudes A, George A, Mukerjee P, Kim JS, Pollet B, Benke PI, Yang F, Mitra P, Sun L, Cetinkol OP *et al.* 2012. Biosynthesis and incorporation of side-chain-truncated lignin monomers to reduce lignin polymerization and enhance saccharification. *Plant Biotechnology Journal* **10**: 609–620.

Foster CE, Martin TM, Pauly M. 2010. Comprehensive compositional analysis of plant cell walls (lignocellulosic biomass) part II: carbohydrates. *Journal of Visualized Experiments* **37**: e1837.

Fu C, Mielenz JR, Xiao X, Ge Y, Hamilton CY, Rodriguez M Jr, Chen F, Foston M, Ragauskas A, Bouton J *et al.* 2011. Genetic manipulation of lignin reduces recalcitrance and improves ethanol production from switchgrass. *Proceedings of the National Academy of Sciences, USA* **108**: 3803–3808.

Funk V, Kositsup B, Zhao CS, Beers EP. 2002. The Arabidopsis xylem peptidase XCP1 is a tracheary element vacuolar protein that may be a papain ortholog. *Plant Physiology* **128**: 84–94.

Gorzsas A, Stenlund H, Persson P, Trygg J, Sundberg B. 2011. Cell-specific chemotyping and multivariate imaging by combined FT-IR microspectroscopy and orthogonal projections to latent structures (OPLS) analysis reveals the chemical landscape of secondary xylem. *The Plant Journal* **66**: 903–914.

Gui J, Liu C, Shen J, Li L. 2014. Grain setting defect1, encoding a remorin protein, affects the grain setting in rice through regulating plasmodesmatal conductance. *Plant Physiology* **166**: 1463–1478.

Gui J, Luo L, Zhong Y, Sun J, Umezawa T, Li L. 2019. Phosphorylation of LTF1, an MYB transcription factor in *Populus*, acts as a sensory switch regulating lignin biosynthesis in wood cells. *Molecular Plant* **12**: 1325–1337.

Gui J, Shen J, Li L. 2011. Functional characterization of evolutionarily divergent 4-coumarate:coenzyme a ligases in rice. *Plant Physiology* **157**: 574–586.

Gui J, Zheng S, Liu C, Shen J, Li J, Li L. 2016. OsREM4.1 interacts with OsSERK1 to coordinate the interlinking between abscisic acid and brassinosteroid signaling in rice. *Developmental Cell* **38**: 201–213.

Hu WJ, Kawaoka A, Tsai CJ, Lung J, Osakabe K, Ebinuma H, Chiang VL. 1998. Compartmentalized expression of two structurally and functionally distinct 4-coumarate:CoA ligase genes in aspen (*Populus tremuloides*). *Proceedings of the National Academy of Sciences, USA* **95**: 5407–5412.

Jin H, Cominelli E, Bailey P, Parr A, Mehrtens F, Jones J, Tonelli C, Weisshaar B, Martin C. 2000. Transcriptional repression by *AtMYB4* controls production of UV-protecting sunscreens in Arabidopsis. *EMBO Journal* **19**: 6150–6161.

Jones L, Ennos AR, Turner SR. 2001. Cloning and characterization of *irregular xylem4* (*irx4*): a severely lignin-deficient mutant of Arabidopsis. *The Plant Journal* **26**: 205–216.

Kern KA, Ewers FW, Telewski FW, Koehler L. 2005. Mechanical perturbation affects conductivity, mechanical properties and aboveground biomass of hybrid poplars. *Tree Physiology* **25**: 1243–1251.

Kumar M, Campbell L, Turner S. 2016. Secondary cell walls: biosynthesis and manipulation. *Journal of Experimental Botany* **67**: 515–531.

Lam PY, Lui ACW, Yamamura M, Wang L, Takeda Y, Suzuki S, Liu H, Zhu FY, Chen MX, Zhang J *et al.* 2019. Recruitment of specific flavonoid B-ring hydroxylases for two independent biosynthesis pathways of flavone-derived metabolites in grasses. *New Phytologist* **223**: 204–219.

Lam PY, Tobimatsu Y, Takeda Y, Suzuki S, Yamamura M, Umezawa T, Lo C. 2017. Disrupting flavone synthase II alters lignin and improves biomass digestibility. *Plant Physiology* **174**: 972–985.

Lapierre C. 1993. Application of new methods for the investigation of lignin structure. In: Jung HG, Buxton DR, Hatfield RD, Ralph J, eds. *Forage cell wall structure and digestibility*. Madison, WI, USA: Wiley, 133–166.

Lapierre C, Monties B, Rolando C. 1986. Preparative thioacidolysis of spruce lignin - isolation and identification of main monomeric products. *Holzforschung* **40**: 47–50.

Leple JC, Dauwe R, Morreel K, Storme V, Lapierre C, Pollet B, Naumann A, Kang KY, Kim H, Ruel K *et al.* 2007. Downregulation of cinnamoyl-coenzyme A reductase in poplar: multiple-level phenotyping reveals effects on cell wall polymer metabolism and structure. *The Plant Cell* **19**: 3669–3691.

Li L, Zhou Y, Cheng X, Sun J, Marita JM, Ralph J, Chiang VL. 2003. Combinatorial modification of multiple lignin traits in trees through multigene cotransformation. *Proceedings of the National Academy of Sciences, USA* **100**: 4939–4944.

Liljegren SJ, Ditta GS, Eshed Y, Savidge B, Bowman JL, Yanofsky MF. 2000. SHATTERPROOF MADS-box genes control seed dispersal in Arabidopsis. *Nature* **404**: 766–770.

Liu CC, Xiao L, Jiang JX, Wang WX, Gu F, Song DL, Yi ZL, Jin YC, Li LG. 2013. Biomass properties from different *Miscanthus species*. *Food and Energy Security* **2**: 12–19.

Mansfield SD, Kim H, Lu FC, Ralph J. 2012. Whole plant cell wall characterization using solution-state 2D NMR. *Nature Protocols* **7**: 1579–1589.

Meents MJ, Watanabe Y, Samuels AL. 2018. The cell biology of secondary cell wall biosynthesis. *Annals of Botany* **121**: 1107–1125.

Meyer K, Shirley AM, Cusumano JC, Bell-Lelong DA, Chapple C. 1998. Lignin monomer composition is determined by the expression of a cytochrome P450-dependent monooxygenase in Arabidopsis. *Proceedings of the National Academy of Sciences, USA* **95**: 6619–6623.

Morreel K, Ralph J, Kim H, Lu F, Goeminne G, Ralph S, Messens E, Boerjan W. 2004. Profiling of oligolignols reveals monolignol coupling conditions in lignifying poplar xylem. *Plant Physiology* **136**: 3537–3549.

Nakashima J, Chen F, Jackson L, Shadle G, Dixon RA. 2008. Multi-site genetic modification of monolignol biosynthesis in alfalfa (*Medicago sativa*): effects on lignin composition in specific cell types. *New Phytologist* **179**: 738–750.

Osakabe K, Tsao CC, Li L, Popko JL, Umezawa T, Carraway DT, Smeltzer RH, Joshi CP, Chiang VL. 1999. Coniferyl aldehyde 5-hydroxylation and methylation direct syringyl lignin biosynthesis in angiosperms. *Proceedings of the National Academy of Sciences, USA* **96**: 8955–8960.

Pauly M, Keegstra K. 2010. Plant cell wall polymers as precursors for biofuels. *Current Opinion in Plant Biology* **13**: 305–312.

Ralph J, Lapierre C, Boerjan W. 2019. Lignin structure and its engineering. *Current Opinion in Biotechnology* **56**: 240–249.

Rao X, Chen X, Shen H, Ma Q, Li G, Tang Y, Pena M, York W, Frazier TP, Lenaghan S *et al.* 2019. Gene regulatory networks for lignin biosynthesis in switchgrass (*Panicum virgatum*). *Plant Biotechnology Journal* **17**: 580–593.

Rao X, Dixon RA. 2018. Current models for transcriptional regulation of secondary cell wall biosynthesis in grasses. *Frontiers in Plant Science* **9**: 399.

Saka S, Hosoya S, Stgermain FGT, Goring DAI. 1988. A comparison of the bromination of syringyl and guaiacyl-type lignins. *Holzforschung* **42**: 79–83.

Schilmiller AL, Stout J, Weng JK, Humphreys J, Ruegger MO, Chapple C. 2009. Mutations in the cinnamate 4-hydroxylase gene impact metabolism, growth and development in Arabidopsis. *The Plant Journal* **60**: 771–782.

Shadle G, Chen F, Srinivasa Reddy MS, Jackson L, Nakashima J, Dixon RA. 2007. Down-regulation of hydroxycinnamoyl CoA: shikimate hydroxycinnamoyl transferase in transgenic alfalfa affects lignification, development and forage quality. *Phytochemistry* **68**: 1521–1529.

Song DL, Gui JS, Liu CC, Sun JY, Li LG. 2016. Suppression of PtrDUF579-3 expression causes structural changes of the glucuronoxylan in *Populus*. *Frontiers in Plant Science* **7**: 493.

Song D, Shen J, Li L. 2010. Characterization of cellulose synthase complexes in *Populus* xylem differentiation. *New Phytologist* **187**: 777–790.

Song D, Sun J, Li L. 2014. Diverse roles of PtrDUF579 proteins in *Populus* and PtrDUF579-1 function in vascular cambium proliferation during secondary growth. *Plant Molecular Biology* **85**: 601–612.

Stewart JJ, Akiyama T, Chapple C, Ralph J, Mansfield SD. 2009. The effects on lignin structure of overexpression of ferulate 5-hydroxylase in hybrid poplar. *Plant Physiology* **150**: 621–635.

Sundell D, Street NR, Kumar M, Mellerowicz EJ, Kucukoglu M, Johnsson C, Kumar V, Mannapperuma C, Delhomme N, Nilsson O *et al.* 2017. AspWood: high-spatial-resolution transcriptome profiles reveal uncharacterized modularity of wood formation in *Populus tremula*. *The Plant Cell* **29**: 1585–1604.

Takata N, Awano T, Nakata MT, Sano Y, Sakamoto S, Mitsuda N, Taniguchi T. 2019. *Populus* NST/SND orthologs are key regulators of secondary cell wall formation in wood fibers, phloem fibers and xylem ray parenchyma cells. *Tree Physiology* **39**: 514–525.

Takeda Y, Koshiba T, Tobimatsu Y, Suzuki S, Murakami S, Yamamura M, Rahman MM, Takano T, Hattori T, Sakamoto M *et al.* 2017. Regulation of CONIFERALDEHYDE 5-HYDROXYLASE expression to modulate cell wall lignin structure in rice. *Planta* **246**: 337–349.

Takeda Y, Tobimatsu Y, Yamamura M, Takano T, Sakamoto M, Umezawa T. 2019. Comparative evaluations of lignocellulose reactivity and usability in transgenic rice plants with altered lignin composition. *Journal of Wood Science* **65**: 6.

Tarmadi D, Tobimatsu Y, Yamamura M, Miyamoto T, Miyagawa Y, Umezawa T, Yoshimura T. 2018. NMR studies on lignocellulose deconstructions in the digestive system of the lower termite *Coptotermes formosanus Shiraki*. *Scientific Reports* **8**: 1290.

Tobimatsu Y, Chen F, Nakashima J, Escamilla-Trevino LL, Jackson L, Dixon RA, Ralph J. 2013. Coexistence but independent biosynthesis of catechyl and guaiacyl/syringyl lignin polymers in seed coats. *The Plant Cell* **25**: 2587–2600.

Tobimatsu Y, Schuetz M. 2019. Lignin polymerization: how do plants manage the chemistry so well? *Current Opinion in Biotechnology* **56**: 75–81.

Umezawa T. 2018. Lignin modification in planta for valorization. *Phytochemistry Reviews* **17**: 1305–1327.

Van Acker R, Leple JC, Aerts D, Storme V, Goeminne G, Ivens B, Legee F, Lapierre C, Piens K, Van Montagu MC *et al.* 2014. Improved saccharification and ethanol yield from field-grown transgenic poplar deficient in cinnamoyl-CoA reductase. *Proceedings of the National Academy of Sciences, USA* **111**: 845–850.

VanAcker R, Vanholme R, Piens K, Boerjan W. 2016. Saccharification protocol for small-scale lignocellulosic biomass samples to test processing of cellulose into glucose. *Bio-protocol* **6**: e1701.

Vanholme R, Cesarino I, Rataj K, Xiao YG, Sundin L, Goeminne G, Kim H, Cross J, Morreel K, Araujo P *et al.* 2013. Caffeoyl shikimate esterase (CSE) is an enzyme in the lignin biosynthetic pathway in Arabidopsis. *Science* **341**: 1103–1106.

Vanholme R, De Meester B, Ralph J, Boerjan W. 2019. Lignin biosynthesis and its integration into metabolism. *Current Opinion in Biotechnology* **56**: 230–239.

Vargas L, Cesarino I, Vanholme R, Voorend W, Saleme MDS, Morreel K, Boerjan W. 2016. Improving total saccharification yield of Arabidopsis plants by vessel-specific complementation of caffeoyl shikimate esterase (cse) mutants. *Biotechnology for Biofuels* **9**: 139.

Venverloo CJ. 1971. Lignin of *Populus nigra* L. cv 'Italica' and some other *Salicaceae*. *Holzforschung* **25**: 18–24.

Voelker SL, Lachenbruch B, Meinzer FC, Jourdes M, Ki C, Patten AM, Davin LB, Lewis NG, Tuskan GA, Gunter L *et al.* 2010. Antisense down-regulation

of *4CL* expression alters lignification, tree growth and saccharification potential of field-grown poplar. *Plant Physiology* **154**: 874–886.

Wang JP, Matthews ML, Williams CM, Shi R, Yang CM, Tunlaya-Anukit S, Chen HC, Li QZ, Liu J, Lin CY *et al.* 2018. Improving wood properties for wood utilization through multi-omics integration in lignin biosynthesis. *Nature communications* **9**: 1579.

Weng JK, Chapple C. 2010. The origin and evolution of lignin biosynthesis. *New Phytologist* **187**: 273–285.

Weng JK, Li X, Bonawitz ND, Chapple C. 2008. Emerging strategies of lignin engineering and degradation for cellulosic biofuel production. *Current Opinion in Biotechnology* **19**: 166–172.

Whetten R, Sederoff R. 1995. Lignin biosynthesis. *The Plant Cell* **7**: 1001–1013.

Wilkerson CG, Mansfield SD, Lu F, Withers S, Park JY, Karlen SD, Gonzales-Vigil E, Padmakshan D, Unda F, Rencoret J *et al.* 2014. Monolignol ferulate transferase introduces chemically labile linkages into the lignin backbone. *Science* **344**: 90–93.

Xi W, Song D, Sun J, Shen J, Li L. 2017. Formation of wood secondary cell wall may involve two type cellulose synthase complexes in *Populus*. *Plant Molecular Biology* **93**: 419–429.

Yamamura M, Hattori T, Suzuki S, Shibata D, Umezawa T. 2012. Microscale thioacidolysis method for the rapid analysis of beta-*O*-4 substructures in lignin. *Plant Biotechnology* **29**: 419–423.

Yang C, Xu Z, Song J, Conner K, Vizcay Barrena G, Wilson ZA. 2007. Arabidopsis *MYB26/MALE STERILE35* regulates secondary thickening in the endothecium and is essential for anther dehiscence. *The Plant Cell* **19**: 534–548.

Yang F, Mitra P, Zhang L, Prak L, Verhertbruggen Y, Kim JS, Sun L, Zheng KJ, Tang KX, Auer M *et al.* 2013. Engineering secondary cell wall deposition in plants. *Plant Biotechnology Journal* **11**: 325–335.

Yue FX, Lu FC, Sun RC, Ralph J. 2012. Syntheses of lignin-derived thioacidolysis monomers and their uses as quantitation standards. *Journal of Agricultural and Food Chemistry* **60**: 922–928.

Zhao Q, Dixon RA. 2011. Transcriptional networks for lignin biosynthesis: more complex than we thought? *Trends in Plant Science* **16**: 227–233.

Supporting Information

Additional Supporting Information may be found online in the Supporting Information section at the end of the article.

Fig. S1 Suppression of lignin biosynthesis by constitutive expression of LTF1AA leads to abnormal growth in *Populus*.

Fig. S2 Identification of vessel-specific and fibre-specific promoters in *Populus*.

Fig. S3 Biomass yield of cell-type-specific suppression of lignin biosynthesis in *Populus*.

Fig. S4 Measurement of mechanical properties of *Populus* stem.

Fig. S5 Suppression of lignin biosynthesis by constitutive expression of LTF1AA leads to abnormal development of xylem vessel and fibre cells.

Fig. S6 Cell-specific overexpression of LTF1AA suppresses lignin biosynthesis in a cell-specific manner of the field-grown trees.

Table S1 List of primers used in this study.

Please note: Wiley Blackwell are not responsible for the content or functionality of any Supporting Information supplied by the authors. Any queries (other than missing material) should be directed to the *New Phytologist* Central Office.